Contents:

Table S1 EDS results: elemental constitution of schwertmannite particles in samples reacted for 6 hours.

Experiment	Fe(At%)	S(At%)	As(At%)	O(At%)
0 ppm, 6 hours	45.15	10.33	-	44.52
10 ppm, 6 hours	26.17	7.07	0.72	65.64
50 ppm, 6 hours	27.63	8	1.68	62.11
100 ppm, 6 hours	33.80	8.76	2.97	54.47
200 ppm, 6 hours	34.97	10.62	5.92	46.95

Table S2 EDS results: elemental constitution of jarosite particles in samples reacted for 6 hours.

Experiment	K(At%)	Fe(At%)	S(At%)	As(At%)	O(At%)
0 ppm, 6 hours	3.99	27.98	13.20	-	54.83
10 ppm, 6 hours	1.57	27.63	8.87	0.39	61.53
50 ppm, 6 hours	3.52	30.16	12.64	1.19	52.48
100 ppm, 6 hours	2.01	32.61	10.91	2.18	52.29
200 ppm, 6 hours	2.73	22.27	10.30	3.44	61.27

Table S3 EDS results: elemental constitution of jarosite particles in samples reacted for 15 hours.

Experiment	K(At%)	Fe(At%)	S(At%)	As(At%)	O(At%)
0 ppm, 15 hours	5.04	23.33	13.17	-	54.83
10 ppm, 15 hours	3.62	18.70	10.42	0.06	67.19
50 ppm, 15 hours	7.07	51.51	13.95	0.14	27.33
100 ppm, 15 hours	6.91	38.32	17.54	0.38	36.85
200 ppm, 15 hours	3.97	13.76	10.41	0.50	71.36

* The EDS data of elemental constitution for schwertmannite and jarosite under different initial coprecipitated As(Ⅲ) concentrations (Tables S1–S3) are the average results of 5 spots for the two kinds of mineral particles with distinguished morphology.

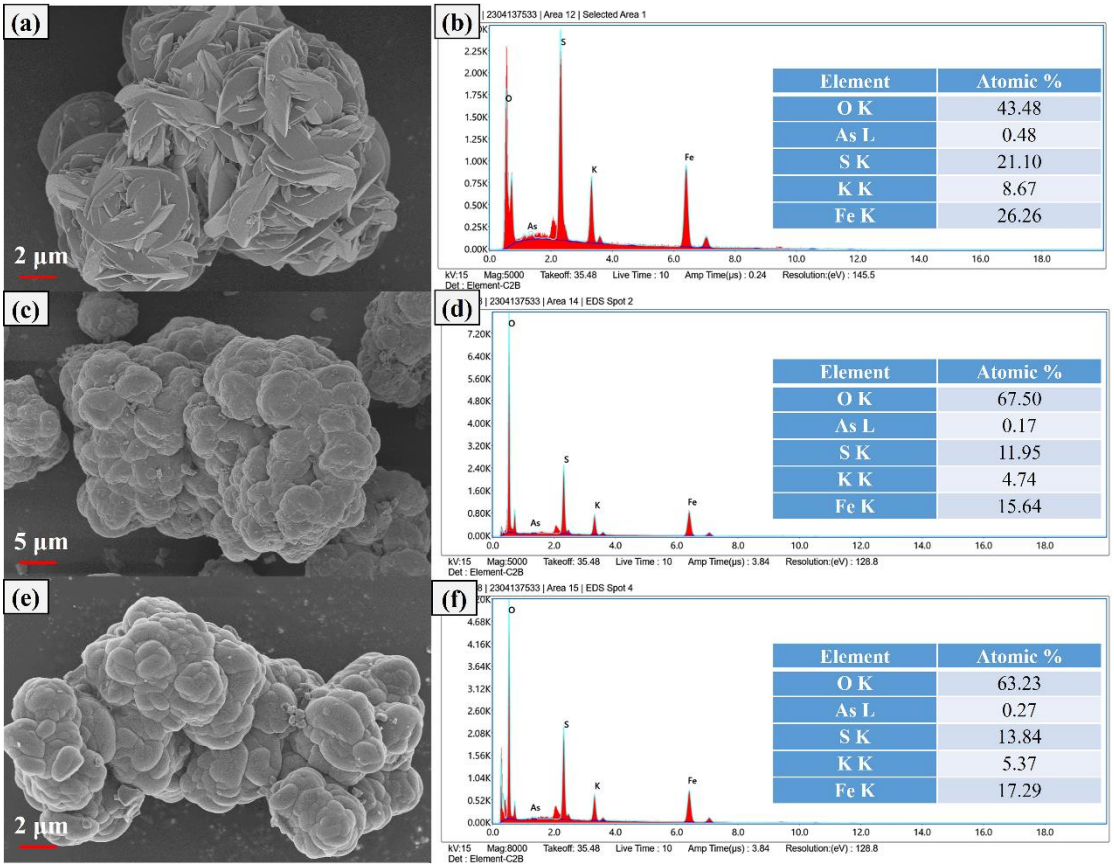

Figure S1 SEM images and corresponding EDS results of precipitated samples collected at 72 h from a biogenic coprecipitation experiment, with the initial bacteria concentrations of 10^7 cells·mL^{-1} (a) and (b), 10^8 cells·mL^{-1} (c) and (d), 10^9 cells·mL^{-1} (e) and (f).

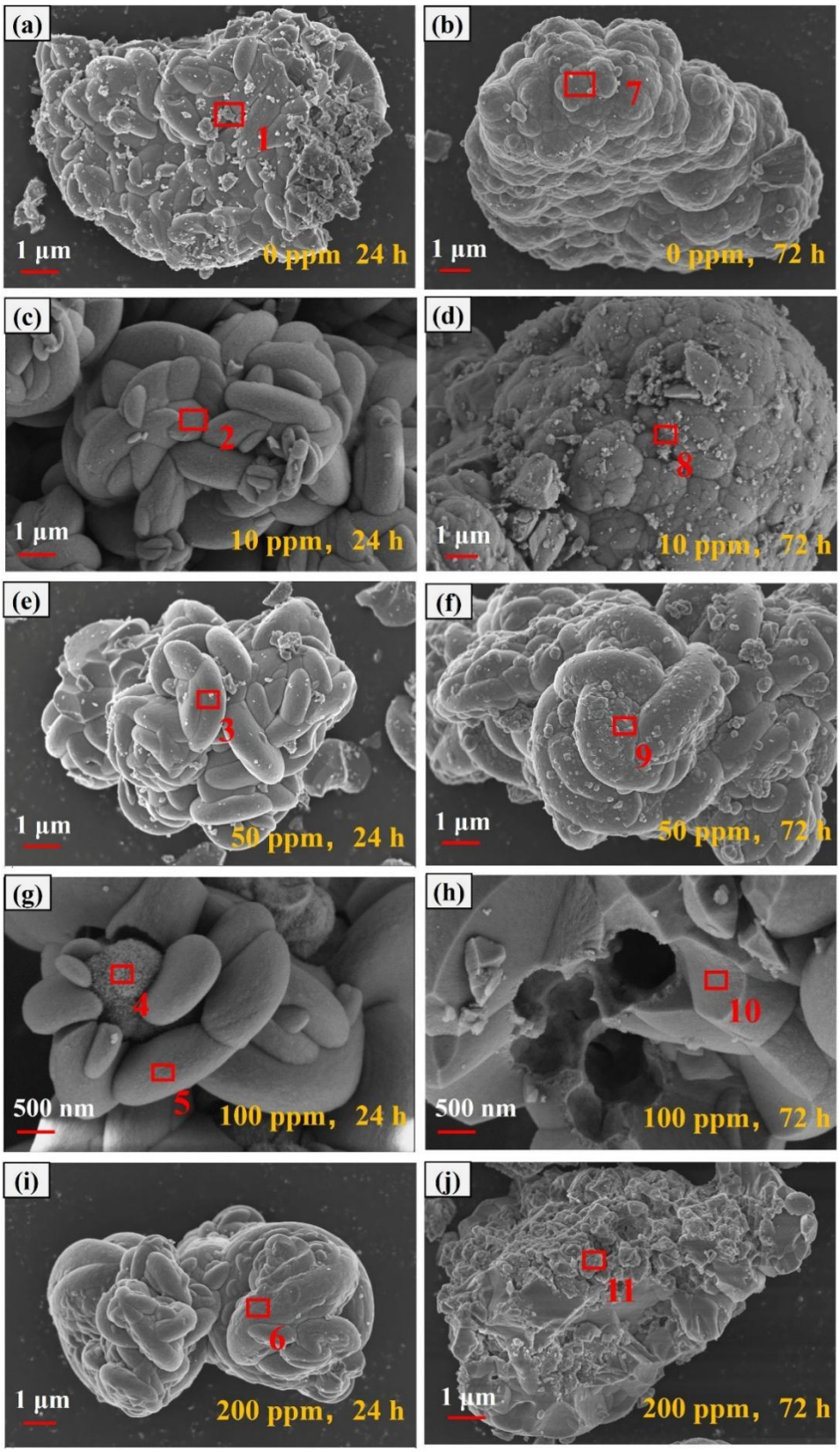

Figure S2 SEM images of precipitated samples collected at 24 h from an experiment with initial As(III) concentrations of 0 ppm (a), 10 ppm (c), 50 ppm (e), 100 ppm (g), and 200 ppm (i); at 72 h from an experiment with the As(III) addition of 0 ppm (b), 10 ppm (d), 50 ppm (f), 100 ppm (h) and 200 ppm (j).

Table S4 EDS results of the local areas marked in Figure S2.

Number	Experiment	K (At%)	Fe (At%)	S (At%)	As (At%)	O (At%)
1	0 ppm, 24 h	6.21	21.73	14.69	-	55.37
2	10 ppm, 24 h	4.55	14.28	11.65	0.17	68.35
3	50 ppm, 24 h	3.43	13.05	9.02	0.33	74.16
4	100 ppm, 24 h	2.78	29.83	11.84	0.59	54.96
5	100 ppm, 24 h	4.29	17.74	12.23	0.40	65.34
6	200 ppm, 24 h	5.67	19.81	14.48	0.31	59.73
7	0 ppm, 72 h	4.81	15.49	13.05	-	67.65
8	10 ppm, 72 h	8.09	26.92	16.45	0.13	48.41
9	50 ppm, 72 h	4.11	13.24	10.81	0.25	71.59
10	100 ppm, 72 h	4.01	18.05	10.54	0.50	66.89
11	200 ppm, 72 h	5.92	23.06	14.96	0.50	52.26

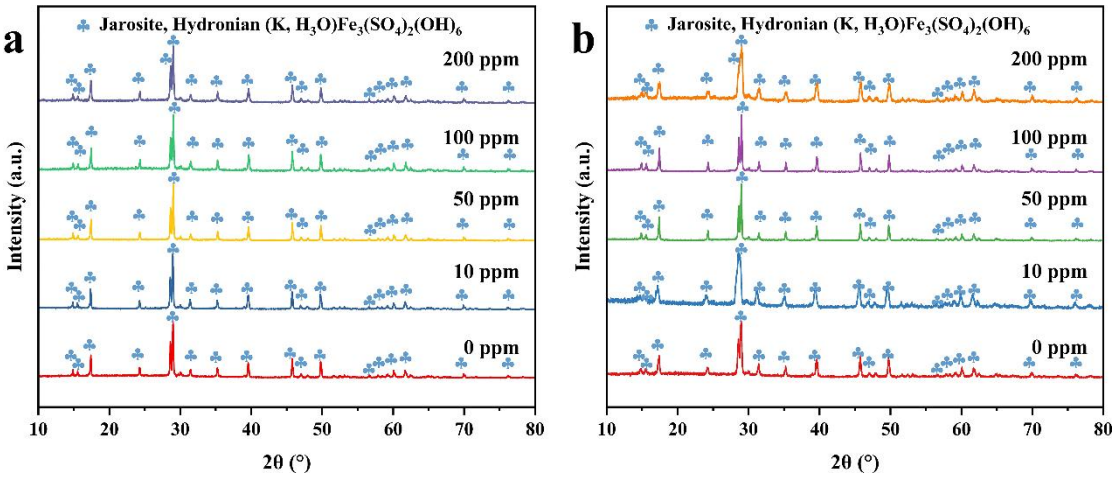

Figure S3 XRD patterns of coprecipitated residue with different initial arsenite concentrations, 24 h (a) and 72 h (b).

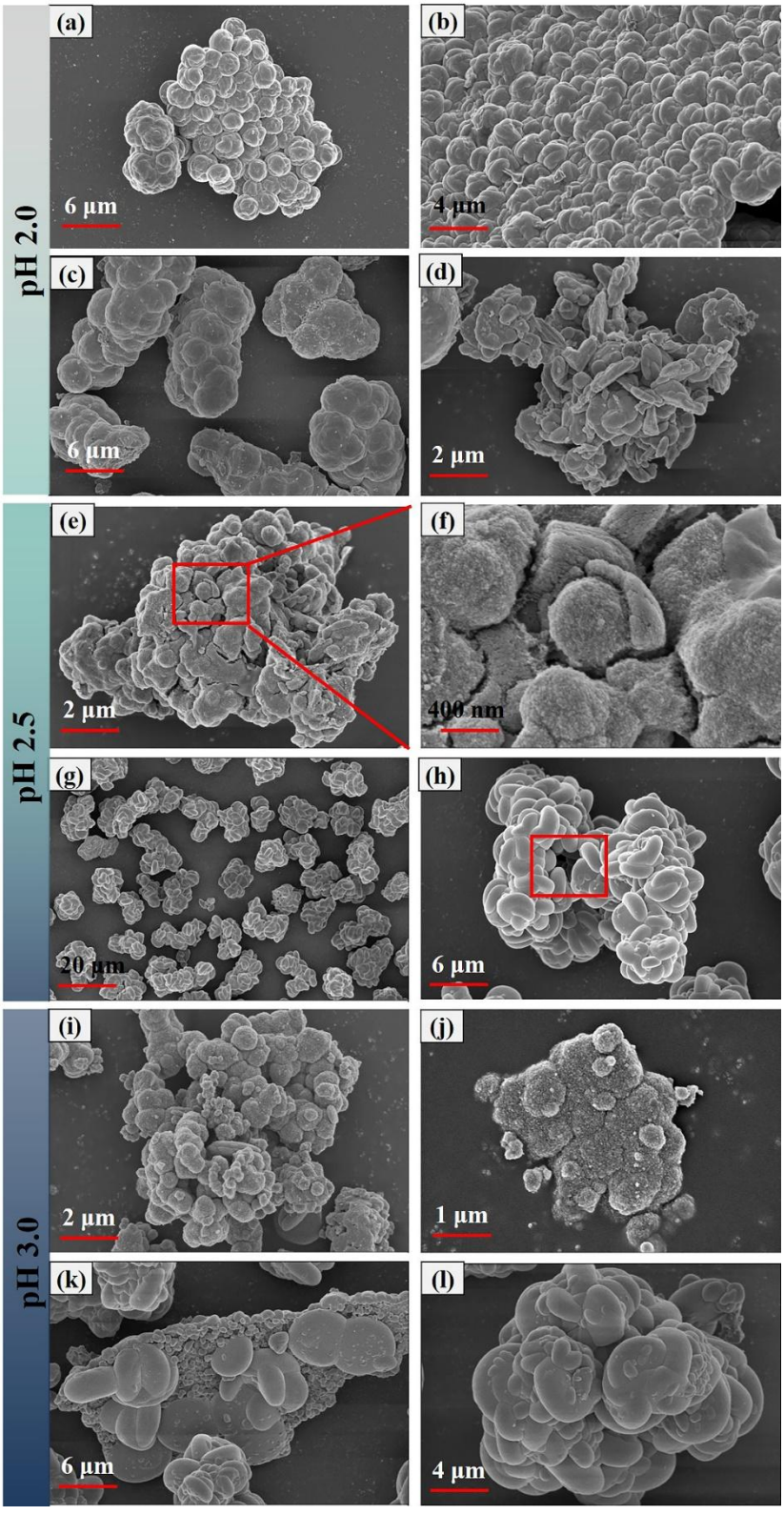

Figure S4 Morphology changes of samples of the three pH experiments during the mineral transformation, pH 2.0, 29 h (a-b), pH 2.0, 72 h (c-d), pH 2.5, 7 h (e-f), pH 2.5, 72 h (g-h), pH 3.0, 7 h (i-j), and pH 3.0, 72 h (k-l).

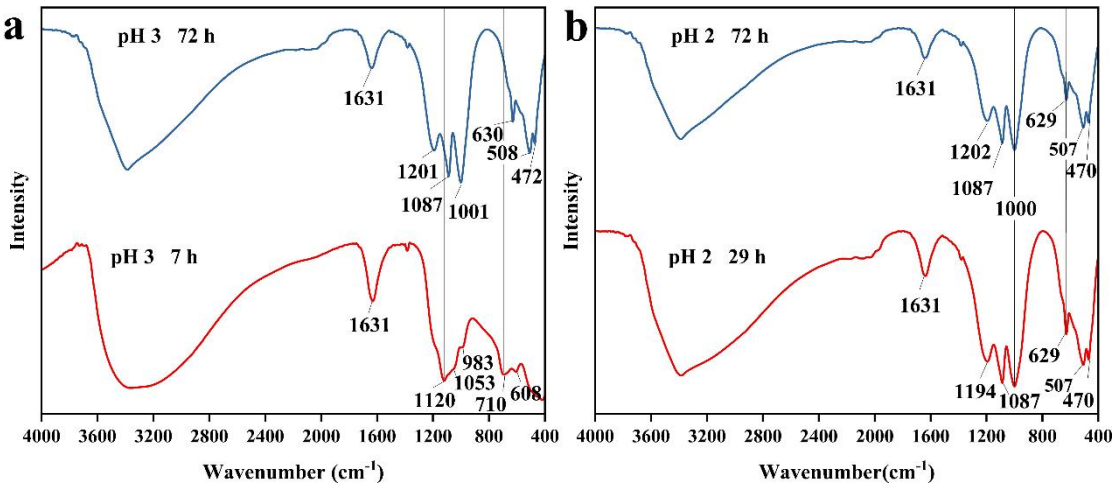

Figure S5 The variation of the FTIR spectra of the initial and late coprecipitation stages of the pH 3.0 group (a) and pH 2.0 group (b).

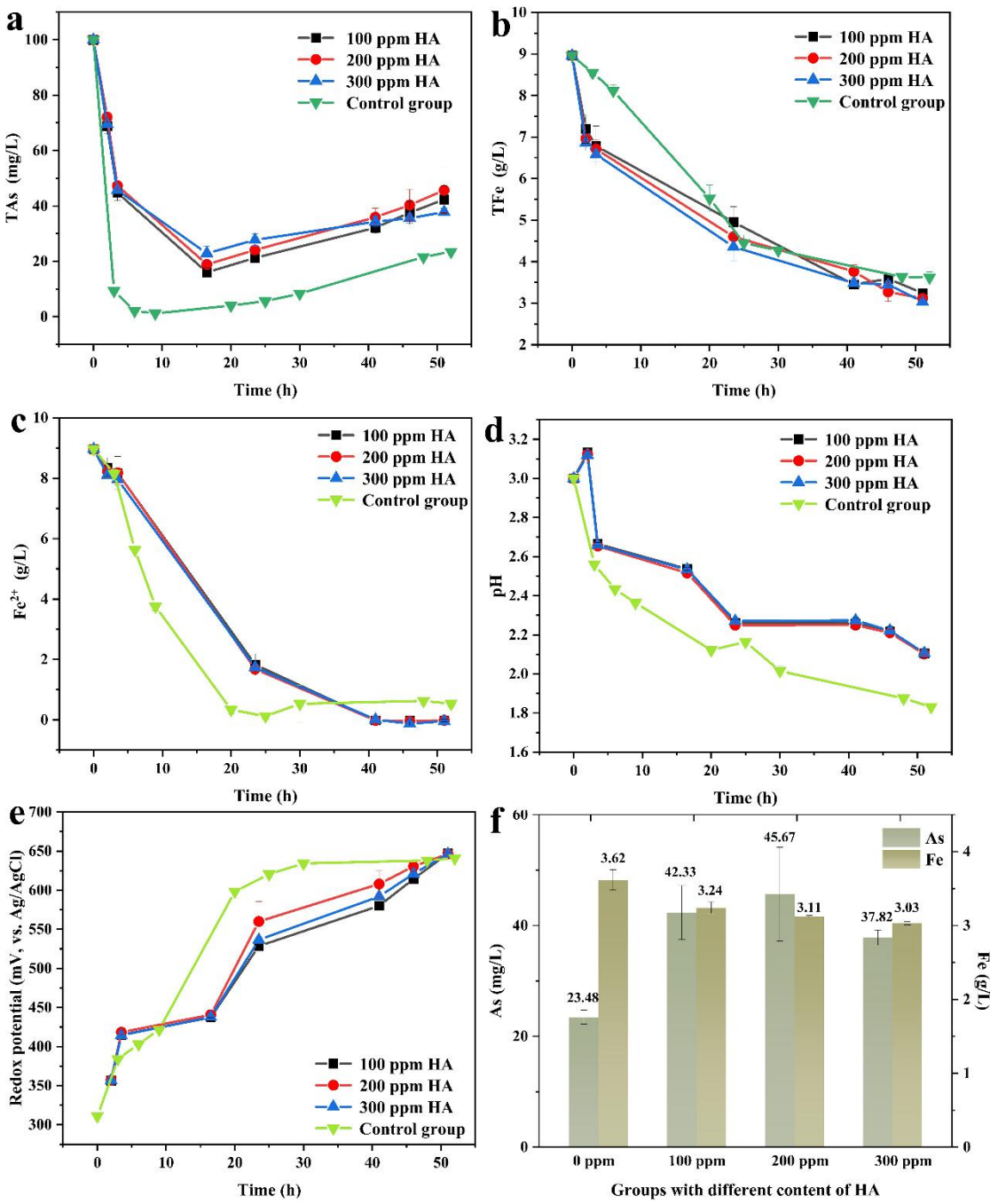

Figure S6 The variation of TAs (a), TFe (b), Fe^{2+} (c), pH (d) and redox potential (e) values with HA addition in jarosite coprecipitation with 100 ppm As(III), and the corresponding column graph comparing residue aqueous As and Fe concentration with the presence of different concentrations of HA after about 50 h (f).

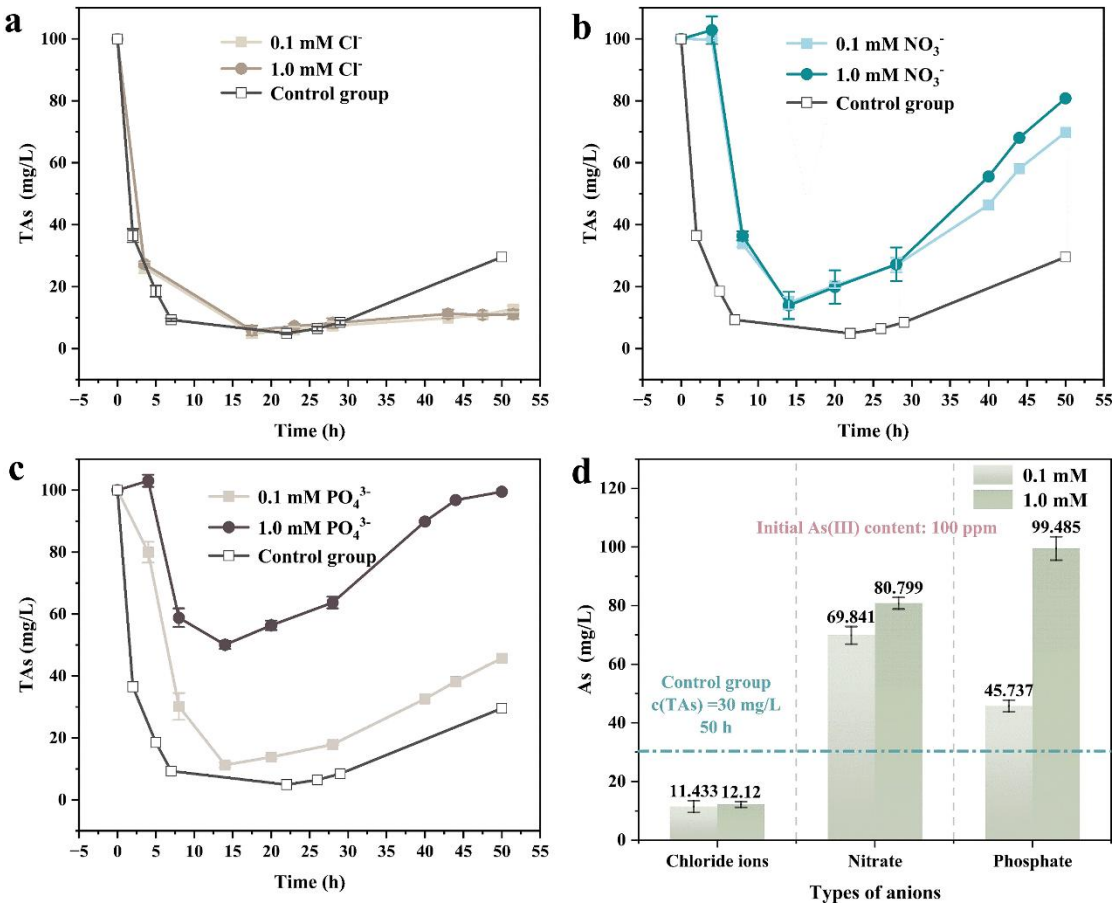

Figure S7 The variation of TAs in experiments with the addition of PO_4^{3-} (a), NO_3^- (b) Cl^- (c) in jarosite coprecipitation with 100 ppm As(III), and the corresponding column graph comparing residue aqueous As concentration with different types of anions after 50 h (d).